Proceedings of the 35th European Safety and Reliability & the 33rd Society for Risk Analysis Europe Conference
Edited by Eirik Bjorheim Abrahamsen, Terje Aven, Frederic Bouder, Roger Flage, Marja Ylönen
 Published by Research Publishing, Singapore.
doi: 10.3850/978-981-94-3281-3_ESREL-SRA-E2025-P2233-cd

Continuous-state survival functions for reinforced concrete bridges based on physics-based degradation models and visual inspection

Francesca Marsili

Chair of Engineering Material and Building Preservation, Helmut-Schmidt-University/University of the Federal Armed Forces Hamburg, Germany. E-mail: francesca.marsili@hsu-hh.de

Niklas R. Winnewisser

Institute for Risk and Reliability, Leibniz University Hannover, Germany.
E-mail: winnewisser@irz.uni-hannover.de

Michael Beer

Institute for Risk and Reliability, Leibniz University Hannover; Institute for Risk and Uncertainty, University of Liverpool; International Join Research Center for Resilient Infrastructure & International Joint Research Center for Engineering Reliability and Stochastic Mechanics, Tongji University.
E-mail: beer@irz.uni-hannover.de

Sylvia Keßler

Chair of Engineering Material and Building Preservation, Helmut-Schmidt-University/University of the Federal Armed Forces Hamburg, Germany. E-mail: sylvia.kessler@hsu-hh.de

This study presents an approach to evaluate the Continuous-State Survival Functions (CSSF) of structural systems, considering the degradation of individual components and their arrangement within the system. System reliability is quantified using the Diagonally Approximated Signature (DAS), a framework that separates the system's topological configuration from the probabilistic behavior of its components, enabling efficient reliability computation. Although traditional survival signature methods assume binary states, this work extends the concept to accommodate continuously degrading components. Component reliability is evaluated through a physics-based degradation model, integrated with results from visual inspections of the structure. The proposed approach is demonstrated on a reinforced concrete girder bridge structure affected by corrosion. The system components - namely the bridge girders - are characterized by different deterioration processes. The DAS acts as a surrogate modeling approach and provides an efficient alternative for costly Monte Carlo simulation. The proposed procedure includes deriving CSSFs for structural elements and then propagating these through the DAS to quantify the CSSFs of the bridge. Thus, this paper constitutes a further stepping stone for stochastically simulating large-scale systems for infrastructure network reliability analyses under various degradation dynamics.

Keywords: Reliability analysis, system analysis, survival signature, Bridge Management System, reinforced concrete, corrosion.

1. Introduction

1.1. *Motivation of the study*

Concrete bridges are critical for transportation and economic activities, but they are subject to increasing damage, the main cause of which is corrosion. Limited resources for maintenance make timely intervention difficult, emphasizing the need for efficient resource allocation. The bridge infrastructure follows a hierarchical structure: at the lower level, structural components deteriorate and threaten the reliability of the object; at the higher level, bridges serve as critical links in road or rail networks, and their failure jeopardizes the functioning of the entire system. Assessing how component deterioration affects overall system performance is critical to optimizing maintenance. Data about bridge condition is managed through Bridge Management Systems (BMS), which store results of visual inspection at different infrastructure levels – damage, component, and bridge.

Condition is assessed on a discrete scale, but data imbalance, with most bridges in good condition, complicates the prediction of future deterioration. To overcome these challenges, condition data can be combined with physical models, such as mechanistic-empirical models for corrosion. These models quantify degradation by linking physical variables to damage progression, improving predictive accuracy.

This paper assesses the reliability of a bridge structure by accounting for the time-dependent degradation of its components and their arrangement within the system. Component degradation is modeled using a physics-based approach, integrated with visual inspection data. Bridge reliability is expressed through a Continuous-State Survival Function (CSSF), extending the survival signature concept to components with continuous states. To efficiently evaluate the CSSF, the Diagonally Approximated Signature (DAS) surrogate modeling approach is employed. The methodology is demonstrated on a reinforced concrete girder bridge affected by corrosion. The paper is organized as follows: in Sec. 2, mechanistic-empirical physical models describing corrosion initiation and progression are presented in Sec. 2.1; the approach to derive CSSF is described in Sec. 2.2. An application of both methods is presented in Sec. 3. Sec. 4 provides an overview of the proposed research and outlines possible future developments.

1.2. *Damage evaluation based on visual inspection*

The SIB-Bauwerke (SIB-BW) database is a key component of Germany's BMS, storing inventory and condition data from periodic visual inspections on bridge structures. Primary inspections occur every six years, with secondary inspections in between.

SIB-BW is structured hierarchically into bridges, components (e.g., superstructure, substructure), and damages. Damages are identified, described by location and extent, and classified into five discrete damage classes (DC 0–4). Condition assessments consider impacts on ultimate, serviceability, and durability limit states, with an algorithm aggregating damage severity and extent at component and bridge levels.

Reinforced concrete bridges are prone to various degradation processes. One of the most well-known processes is corrosion, which manifests as concrete spalling and exposed, corroded rebars. Corrosion can be modeled using partial differential equations. Specifically, analytical models can be derived for the time of corrosion initiation and its progression.

As corroded rebars expand in volume, they cause the concrete cover to crack. A key physical parameter for describing corrosion progression is the width of the crack resulting from corrosion products on the concrete surface. A correspondence can be established between the DC assigned during visual inspection to concrete cover cracking and spalling and the output parameters of mechanistic-empirical degradation models. A qualitative description of the evaluation process based on visual inspections and the corresponding DC is presented in Table 1. This table serves as a reference for inspectors to assess damage. It also illustrates the relationship between the qualitative evaluation of the DC and the output parameter of the mechanistic-empirical model. An interval of values for the physical parameter can be identified, which corresponds to a specific DC.

Table 1.: Damage classes in SIB-BW to assess the degradation due to corrosion and related values of the physical parameter considered, i.e., crack width on the concrete cover due to corrosion products.

DC	Description	Physical parameter	Values range
0	No damage / Chloride contamination	/	/
1	Corrosion initiation, cracking	Crack width w	$0.05 < w < 0.4$
2	Corrosion propagation, cracking	Crack width w	$0.4 < w < 0.8$
3	Concrete cover spalling	Crack width w	$0.8 < w < 1.2$
4	Advanced corrosion	Rebar diameter reduction Φ_{red}	$\Phi_{red} > 15\%$

2. Methods

2.1. *Mechanistic-empirical model for chloride induced corrosion*

Mechanistic-empirical deterioration models for reinforced concrete (r.c.) elements were established as part of the DuraCrete project DuraCrete (2000) and serve as the basis for the probabilistic durability design of r.c. structures (fib (2006)). Assuming that corrosion is due to the presence of chloride, the time of corrosion initiation t_i can be computed in the following way

$$t_i = \left[\frac{2}{x_c} \cdot erf^{-1}\left(1 - \frac{C_{cr}}{C_s}\right)\right]^{-2} \cdot \cdot \left(\frac{1}{D_0 f_T(t) f_{RH}(t) K_e K_t K_c t_0^n}\right)^{\frac{1}{1-n}} \quad (1)$$

where x_c is the the concrete cover in mm, C_{cr} is the critical chloride concentration, C_s is the surface chloride concentration, D_0 the empirical chloride diffusion coefficient in $mm^2/year$, K_e is the environmental factor, K_c is the curing factor, K_t is the test method factor, t_0 is the age of the concrete when the compliance test is performed in $years$, n is the age factor. $f_T(t)$ is the temperature effect on diffusion coefficient (Stewart et al. (2011))

$$f_T(t) = \exp\left[\frac{E}{R}\left(\frac{1}{293} - \frac{1}{273 + T_{av}(t)}\right)\right] \quad (2)$$

where $E = 40\ kJ/mol$ is the activation energy of the diffusion process, $R = 8.31410^3\ kJ/molK$ is the gas constant and $T_{av}(t)$ is the average temperature at year t. $f_R H(t)$ is the the influence of relative humidity on diffusion coefficient

$$f_{RH}(t) = \exp\left[1 - \frac{(100 - RH_{av}(t))^4}{(100 - 75)^4}\right]^{-1} \quad (3)$$

where $RH_{av}(t)$ is the is the average relative humidity at year t.

C_s is the surface chloride concentration, which depends on the exposure category of the structural element, i.e. submerged, splash, tidal, and atmospheric zone, and it is described by the following expression (DuraCrete (2000))

$$A_{cl}\frac{w}{b} + \varepsilon_{cl} \quad (4)$$

where A_{cl} is a regression coefficient, $\frac{w}{b}$ is the the water to cement ratio and ε_{cl} is an error term.

Corrosion of steel reinforcement begins when the chloride concentration exceeds the critical threshold C_{cr}. This process produces corrosion products that expand, taking up more volume than the original steel rebar. As a result, the concrete cover develops cracks, which may eventually lead to spalling. The width of the cracks is determined in the following way

$$w(t) = w_0 + b\left[p(t) - p_0\right] \quad (5)$$

where w_0 is the initial width of the visible crack in mm, b is the parameter which controls the propagation and depends on the position of the rebar in $mm/\mu m$, p_0 is the value of the corrosion penetration necessary to produce a crack in μm, $p(t)$ is the corrosion penetration at time t in μm. The corrosion penetration p_0 needed to open a crack can be assessed in the following way

$$p_0 = a_1 + a_2\frac{x_c}{d} + a_3 f_{ct} \quad (6)$$

where a_1, a_2, a_3 are regression parameters, x_c is the concrete cover depth in mm, d is the diameter of the steel rebar in mm, f_{ct} is the concrete tensile strength in N/mm^2. The corrosion penetration at time t, $p(t)$, is evaluated as

$$p(t) = i_{corr}(t) w_t (t - t_i) \quad (7)$$

where w_t is the relative time of wetness; t_i is the time to corrosion initiation; $i_{corr}(t)$ is the corrosion rate at time t in mm/year, which depends on temperature and is estimated starting from the value at $20°C$ ($i_{corr,20}$) as

$$i_{corr}(t) = i_{corr,20}\left[1 + K\left(T(t) - 20\right)\right]. \quad (8)$$

2.2. *Continuous-State Survival Function*

This section outlines basic concepts for modeling and assessing engineering systems. The concepts of survival signature in the binary-state consideration and the DAS in the continuous-state case enhance computational efficiency when probabilistic system behavior is evaluated for various scenarios. Further, the CSSF is recalled, which is central to the work presented in this paper.

State vector: Consider a system as a collection of components connected in a specific arrangement and intended to perform a specific task. Both the system's state and the components' state can be represented by a) binary-, b) multi-, or c) continuous-state variables, where either two, a finite, or infinite number of states are allowed: 1) complete functioning (1), 2) complete failure (0), and potentially 3) intermediate levels of functionality. The state vector describes the operational status of the system's components. Traditionally, it is a vector $x = (x_1, x_2, \ldots, x_n) \in \{0, 1\}^n$ for a system comprising n components, where for each component i, $x_i = 1$ if this component is working and $x_i = 0$ if it is not working (Rausand and Hoyland (2003)).

Structure function: The operational state of the system as a whole is a function of the components' states. The structure function is defined as a) $\phi : \{0, 1\}^n \rightarrow \{0, 1\}$ in the binary case, b) $\phi : \{0, s_1, s_2, ..., 1\}^n \rightarrow \{0, s_1, s_2, ..., 1\}$ from the multi-state perspective, and c) $\phi : [0, 1]^n \rightarrow [0, 1]$ for the continuous-state consideration. It indicates the working state of the system given a state vector depending on the modeling perspective a), b), or c) Winnewisser et al. (2023). The modeling perspectives a) and c) are the most significant ones. Firstly, b) can be constructed by combining multiple binary structure functions. Secondly, c) acts as a generalization of a) and b) and can be reduced to both representations accordingly. In fact, for numerical methods in time-dependent considerations, c) typically has to be discretized in time and space, resulting in b).

Coherent system: An important class of systems is known as coherent systems. A system is coherent if the structure function ϕ is monotone and non-decreasing, i.e., $\phi(x) \leq \phi(y)$ if $x \leq y$, and there are no irrelevant components, i.e., each component influences the system performance at some point (Rausand and Hoyland (2003)).

This study restricts the analysis to coherent systems, i.e., coherent structure functions. Nevertheless, this is a realistic assumption, as decreasing the functionality of components should not increase the system's functionality from an engineering perspective.

Continuous-state reliability analyses: In this case, consider the binary-state structure function $\phi(\boldsymbol{x}) : \{0, 1\}^n \rightarrow \{0, 1\}$ to describe the system topology. This requires setting functional thresholds that differentiate between the working and non-working states of components and the overall system. The structure function can be established based on Reliability Block Diagrams (RBD) that incorporate logical operators, such as and- and or-statements. As an alternative, thresholds can be applied to more complex simulation models mapping component variables to the system performance. Given the probabilistic properties as Cumulative Distribution Functions (CDF) $F_{\mathbf{x}}(t)$ that characterize time-dependent failure events of all components, the survival function of the system $R_\phi(t)$ can be computed as $R_\phi(t) = P(\phi(\mathbf{x}) = 1|\mathbf{x} \sim F_{\mathbf{x}}(t))$. Thereby, a failure event considers a transition of a component or system state from 1 to 0. Thus, the survival function of the system is the probability that the system works at time $t > 0$, and it can be calculated based on the structure function (Rausand and Hoyland (2003)).

Similarly, the CSSF is informative when engineers are challenged for more comprehensive reliability analyses. It is denoted as $R_u(s,t)$ and quantified as the probability $P(T_u \geq t|s)$ that the random variable T_u characterizing the random failure time of some entity u is greater or equal to time $t \in R^+$ for a given state $s \in [0,1]$. This is strongly related to the so-called continuous-state reliability of this entity, defined as $R_u(s,t) = P(S_u \geq s|t)$ for the random entity state S_u. Note that $R_u(s,t) = P(T_u \geq t|s) = P(S_u \geq s|t)$ in the case when $R_u(s,t)$ is monotonically decreasing, e.g., for monotonically increasing degradation processes. This aligns with the binary-state survival function defined as $R_u(t) = 1 - CDF_u(t)$, a time-dependent reliability measure for monotonically decreasing processes assuming a single state threshold. Computing the CSSF of a system requires the definition of a continuous-state structure function. Thus, consider $R_\phi(s|t) = P(\phi(\boldsymbol{x}) \geq s)$. In a numerical scheme, the time and state domains are discretized.

Continuous-state survival signature: In Winnewisser et al. (2023) the Diagonally Approximated Signature (DAS) was introduced to exactly compute or at least find a lower bound for the CSSF of a system given its continuous-state structure function. Based on Winnewisser et al. (2024), the fundamental formula for systems with K component types can be stated as

$$R_\phi(s,t) = \sum_{l_s=1}^{n} \sum_{p=1}^{\mathcal{P}(l_s)} \prod_{k=1}^{K} [R_{x_k}(s|t)]^{l_{s,k}} \cdot [R_{x_k}(\Phi(s,l_{s,k},p)|t) - R_{x_k}(s|t)]^{n_k - l_{s,k}}, \quad (9)$$

where l_s is the number of components working in or above state s, $l_{s,k}$ is the number of components of type k working in state s, $\mathcal{P}(l_s) = \binom{n}{l_s}$ represents the number of possible permutations given l_s and is equal to the binomial coefficient, and $R_{x_k}(s|t)$ is the CSSF value of component type $k \in \{1,2,...,K\}$. Further, $\Phi(s,l_{s,k},p)$ is the fundamental form of the DAS. Its assignments for state s, l_s, and permutation $p \in 1,2,...,\mathcal{P}(l_s)$ are the minimum values s^* fulfilling $\phi(s^*) \geq s$ along the diagonals of subspaces $\Omega_{s,l_s,p} \subset \Omega = \{\phi(\boldsymbol{x}) \geq s\}$. The permutations of the vector (x_a, x_b) with $a \in \{i|x_i \geq s\}$ and $b \in \{i|x_i < s\}$ for $i \in 1,2,...,n$ define these diagonals.

Aggregation of $\Phi(s,l_{s,k},p)$ in terms of component types and values in close neighborhoods are discussed in Winnewisser et al. (2024) and enable significant computational efficiency for analyses requiring repeated model evaluation. The accuracy depends on specific properties of the continuous-state structure function discussed in Winnewisser et al. (2023). The concept of DAS achieves accurate results for structure functions that are evaluated in comparable multi-state and continuous-state literature, see Eryilmaz and Tuncel (2016) and Liu et al. (2018), respectively. Further, the DAS extends the applicability of the beneficial separation property, initially introduced in Coolen and Coolen-Maturi (2012) with the concept of survival signature, to continuous-state structure functions that are not diagonal state neutral and extreme. For example, structure functions based on series- and parallel or min- and max-operators are diagonal state neutral and extreme; see discussions in the DAS literature.

3. Application

3.1. *Introduction*

An application of the proposed approach is demonstrated using a reinforced concrete bridge structure affected by corrosion. The structure is a slab bridge that is simply supported by two girders. Figures 1 illustrates the longitudinal static system of the bridge and the cross section. In the cross section, the static system can be modeled as a series system characterized by two components, namely the two girders.

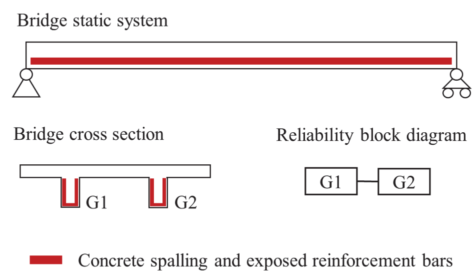

Fig. 1.: Bridge static system and cross section, with areas of concrete spalling and exposed rebars highlighted.

Table 2.: Results of visual inspections carried out on the r.c. girder bridge.

Year	Location	Damage	DC (DLS)	DC (ULS)
2018	Girder 1	Corrosion	1	3
2024	Girder 1	Corrosion	1	3
2018	Girder 2	/	0	/
2024	Girder 2	Corrosion	2	3

The bridge, built in 1979, underwent visual inspections in 2018 and 2024, revealing corrosion in its girders. Damage includes concrete spalling and exposed rebars, varying between girders (Table 2). The first girder received a DC of 1 in both inspections, while the second had no recorded damage in 2018 (DC 0) but was rated DC 2 in 2024. Concrete spalling and exposed rebars reduce bending resistance, affecting structural safety. Parmiani and Orta (2022) found that when exposed reinforcement spans 63% of a beam's length, ultimate moment capacity drops by 12%, with similar findings in Cairns and Zhao (1993). This study assumes resistance reduction depends on both exposed reinforcement length and time. Using mechanistic-empirical models (Section 2.1), a 15% reduction is estimated, represented by a coefficient K_d, where $K_d = 1$ indicates sufficient reliability and $K_d = 0.85$ insufficient reliability.

3.2. *Approach to integrate physics-based model for corrosion progression and results of visual inspection*

Table 3.: PDFs for the parameters of the mechanistic-empirical model describing corrosion initiation and propagation.

Parameter	Mean	St. Dev.	Dist	Unit
C_{cr}	0,5	0,05	N	[%]
x_c	3,3326	0,1371	LN	$[mm]$
A_{cl} (atm)	2,565	0,356	N	[%]
ε_{cl} (atm)	0	0,405	N	[%]
k_e (atm)	0,676	0,114	Ga	[-]
k_t	0,832	0,024	N	[-]
k_c	1	-	Det	[-]
D_0	473	43,2	N	$[mm2/year]$
t_0	0,0767	-	Det	$[year]$
n	0,3	0,12	B	[-]
w_0	0,05	0,005	N	$[mm]$
b	-4,8916	0.2712	LN	$[mm/\mu m]$
a_1	74,4	3,2	N	$[\mu m]$
a_2	7,3	0,06	N	$[\mu m]$
a_3	-17,4	5,7	N	$[\mu m/Mpa]$
f_{ct}	$0.53\sqrt{f_c}$	$0.08\sqrt{f_c}$	N	$[MPa]$
w_t	0,75	0,2	N	[-]
d	60	6	N	$[mm]$
i_{corr}	0,03	0,02	W	$[mm/year]$
$K(T > 20°)$	0,073	0,015	N	[-]
$K(T < 20°)$	0,025	0,005	N	[-]

Based on the correspondence between DC and the width of the crack caused by corrosion outlined in Table 1, approaches can be developed to integrate the results of visual inspections with predictions of damage evolution derived from physics-based models. A possible approach consists of the following steps: 1) Perform a Monte Carlo simulation to generate degradation paths based on the mechanistic-empirical model; 2) For each degradation path, if the physical parameter at time t lies within the range associated with the visual inspection DC, retain this degradation path as a compatible path; 3) For each time step t, randomly sample a value of the physical parameter from the set of compatible degradation paths at t. If the value at $t + 1$ is lower than the value at t, set the value at $t + 1$ equal to the value at t (ensuring non-decreasing behavior). The output is represented by a sampled degradation path that integrates visual inspection data with model predictions. This approach provides a means to account for uncertainty in the degradation process and incorporates information from both visual inspections and mechanistic-empirical models, thereby enhancing the robustness of the damage assessment process.

Table 3 shows the PDF for the input parameters of the mechanistic-empirical models which have been considered to perform the Monte Carlo simulation. Fig. 2 and 3 visualize the degradation paths which are compatible with the results of the visual inspections for girder 1 and girder 2, respectively, and the sampled degradation paths from the compatible degradation paths.

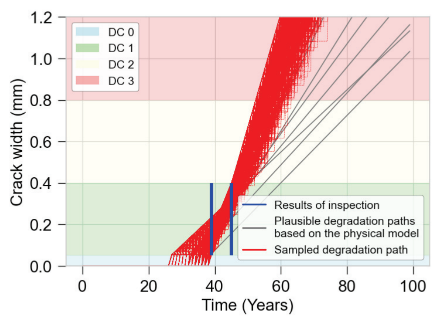

Fig. 2.: Degradation paths for girder 1.

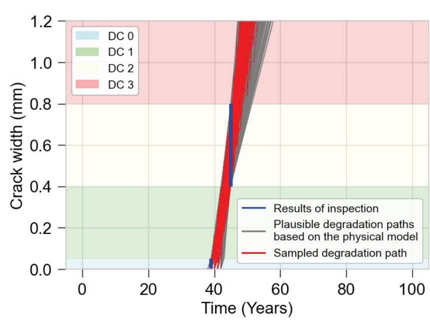

Fig. 3.: Degradation paths for girder 2.

3.3. *Assessment of the continuous-state survival function*

The CSSF characterizing the degradation of the structural elements is computed based on the degradation paths generated as explained in Section 3.2. To probabilistically quantify the state variable x_i for structural component i with $i = 1, 2, ..., n$ in terms of degradation, compute its CSSF as

$$R_{x_i}(s|t) = E[I[\boldsymbol{x}_i(t) \geq s]] \\ = \frac{1}{N}\sum_{j=1}^{N} I[x_{i,j}(t) \geq s], \quad (10)$$

where $\boldsymbol{x}_i(t)$ is the vector containing all samples of x_i at time step t. Following Eq. 10, Fig. 4

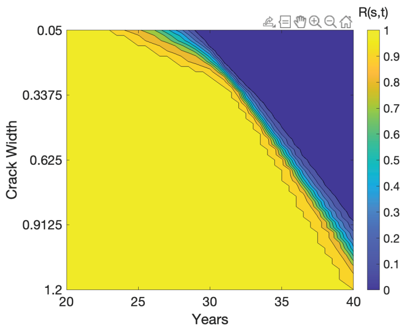

Fig. 4.: Continuous-state survival function for girder 1.

shows the CSSFs of girder 1 regarding damage classes DC, characterizing crack width. In accordance with the continuous-state system modeling as $\phi(\boldsymbol{x}) : [0, 1]^n \rightarrow [0, 1]$, consider normalized states as $s \in [0, 1]$. For each field of application, it is essential to identify a mapping between the measurable or computable variable and the corresponding state variable x_i for component i. In the current case, a direct mapping was chosen to link the crack width c_i to the state interval $x_i \in [0, 1]$

$$x_i = \begin{cases} 1, & \text{if } c_i < 0.05 \\ \frac{0.05 - c_i}{1.15} + 1, & \text{if } 0.05 \geq c_i \leq 1.2 \\ 0 & \text{if } c_i > 1.2 \end{cases}$$

Then, Fig. 5 shows $R_{x_i}(s|t)$ of girder 2.

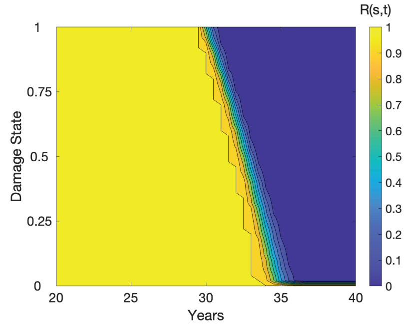

Fig. 5.: Continuous-state survival function for girder 2.

Given a continuous-state structure function characterizing the overall bridge system state depending on the states of its structural components, a CSSF can be computed that represents the bridge safety regarding its degradation. In these terms, a structure function composed of min- and max-operators is a reasonable model assumption. Thereby, the min-operator corresponds to a series connection from a binary-state perspective, while the max-operator corresponds to a parallel connection. In the case of two critical structural elements without redundancy only min-operators are appropriate. Thus, consider $\phi(\boldsymbol{x}) = \min(x_1, x_2, ..., x_n) \in [0, 1]$ for a system with n components and component states $x_i \in [0, 1]$. Note that $\phi(\boldsymbol{x})$ can also be evaluated based on a more complex simulation model that accounts for the structural integrity of the overall structure depending on degrading material parameters of structural elements. For simplicity, the current work is limited to a structure function in the form of $\min(x_1, x_2, ..., x_n)$.

The CSSF $R_\phi(s|t)$, probabilistically representing the safety of the considered bridge, can be computed based on the specified $R_{x_i}(s|t)$ and a reasonable structure function, given as $\phi(\boldsymbol{x}) = \min(x_1, x_2) \in [0, 1]$. For this $\phi(\boldsymbol{x})$, the CSSF for bridge safety can be computed as

$$R_\phi(s|t) = \sum_{l_s=2}^{n=2} \sum_{p=1}^{\mathcal{P}(l_s)=1} \prod_{k=1}^{K=2} [R_{x_k}(s|t)]^{l_{s,k}} \\ = R_{x_1}(s|t) \cdot R_{x_2}(s|t) \\ = P(X_1 \geq s|t) \cdot P(X_2 \geq s|t). \quad (11)$$

These equations are based on the concept of DAS, described in Subsec. 2.2. In fact, for $\phi(\boldsymbol{x}) = \min(x_1, x_2, ..., x_n)$, $R_\phi(s|t) = \prod_{k=1}^{K} \left[R_{x_k}(s|t)\right]^{l_{s,k}}$, in accordance to Eq. 9. This comes from $\Phi(s, l_{s,k}, p) = s$ for each s, $l_{s,k}$, and p when considering $\min(x_1, x_2, ..., x_n)$. Consequently, $\left[R_{x_k}(\Phi(s, l_{s,k}, p)|t) - R_{x_k}(s|t)\right]^{n_k - l_{s,k}}$ reduces to zero as in Eq. 11.

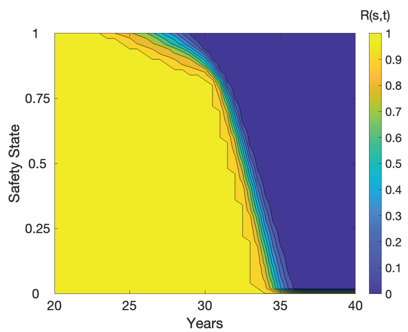

Fig. 6.: Continuous-state survival function for the bridge.

4. Conclusions

This paper presents a methodology to evaluate CSSFs for structural systems. The methodology is based on an extension of the concept of survival signature to systems with continuous degradation states. The concept of DAS provides a generalized perspective and is employed to enhance computational efficiency. This enables accurate reliability assessment for a set of continuous-state systems considered in conventional approaches and provides a lower bound for more complex system topologies. The case study, evaluating a reinforced concrete girder bridge affected by corrosion, where girders exhibit distinct deterioration patterns, demonstrates the applicability of the approach. Time-dependent component degradation is modeled through the integration of the physics-based degradation model and visual inspection results. The work demonstrates the method's potential for efficient reliability evaluation in aging infrastructure to facilitate simulation-based decision-making.

Acknowledgement

The German Research Foundation (DFG) funded this research, as part of the Priority Program SPP 100+ (subproject D01, grant number 2388 501624329). This research project is funded by dtec.bw – Digitalization and Technology Research Center of the Bundeswehr which we gratefully acknowledge. dtec.bw is funded by the European Union – NextGenerationEU.

References

Cairns, J. and Z. Zhao (1993). Behaviour of concrete beams with exposed reinforcement. *Proc Inst Civil Eng Struct Build 99(2)*, 141–54.

Coolen, F. P. A. and T. Coolen-Maturi (2012). Generalizing the signature to systems with multiple types of components. In W. Zamojski, J. Mazurkiewicz, J. Sugier, T. Walkowiak, and J. Kacprzyk (Eds.), *Complex Systems and Dependability*, Berlin, Heidelberg, pp. 115–130. Springer Berlin Heidelberg.

DuraCrete (2000). *Probabilistic performance-based durability design of concrete structures. EU-brite EuRam III.* Project BE95-1347/R9.

Eryilmaz, S. and A. Tuncel (2016). Generalizing the survival signature to unrepairable homogeneous multi-state systems. *Naval Research Logistics (NRL) 63*(8), 593–599.

fib (2006). *fib Bulletin 34, Model Code for Service Life Design*.

Liu, Y., Y. Shi, X. Bai, and B. Liu (2018). Stress–strength reliability analysis of multi-state system based on generalized survival signature. *Journal of Computational and Applied Mathematics 342*, 274–291.

Parmiani, M. and L. Orta (2022). Reliability assessment of a continuous bridge beam with exposed reinforcement. *Engineering Structures 262*, 114281.

Rausand, M. and A. Hoyland (2003). *System reliability theory: models, statistical methods, and applications*, Volume 396. John Wiley & Sons.

Stewart, M. G., X. Wang, and M. N. Nguyen (2011). Climate change impact and risks of concrete infrastructure deterioration. *Engineering Structures 33*(4), 1326–1337.

Winnewisser, N. R., J. Salomon, M. Broggi, and M. Beer (2023). The concept of diagonal approximated signature: new surrogate modeling approach for continuous-state systems in the context of resilience optimization. *Disaster Prevention and Resilience 2*(2), N–A.

Winnewisser, N. R., J. Salomon, Y. Shi, M. Broggi, and M. Beer (2024). Generalizing the diagonal approximated signature to systems with multiple component types. In M.-M. Kolowrocki (Ed.), *Advances in Reliability, Safety and Security*, Gdynia, pp. 199–208. Polish Safety and Reliability Association.